Hindawi
Journal of Chemistry
Volume 2021, Article ID 9986158, 11 pages
https://doi.org/10.1155/2021/9986158

Research Article

Fabrication of Titanium Dioxide/Carbon Fiber (TiO_2/CF) Composites for Removal of Methylene Blue (MB) from Aqueous Solution with Enhanced Photocatalytic Activity

Hao Cheng,[1,2,3] **Wenkang Zhang**,[1] **Xinmei Liu**,[1] **Tingfan Tang**,[1] **and Jianhua Xiong**[2]

[1]*Guangxi Key Laboratory of Green Processing of Sugar Resources, College of Biological and Chemical Engineering, Guangxi University of Science and Technology, Liuzhou 545006, Guangxi, China*
[2]*Guangxi Key Laboratory of Clean Pulp & Papermaking and Pollution Control, College of Light Industry and Food Engineering, Guangxi University, Nanning 530004, Guangxi, China*
[3]*Province and Ministry Co-sponsored Collaborative Innovation Center of Sugarcane and Sugar Industry, Nanning 530004, Guangxi, China*

Correspondence should be addressed to Jianhua Xiong; happybear99@126.com

Received 17 March 2021; Revised 12 May 2021; Accepted 22 May 2021; Published 17 June 2021

Academic Editor: Andrea Petrella

TiO_2 powder was firstly synthesized and carbon fiber was secondly prepared via the carbonization of polyaniline fiber, and TiO_2/carbon fiber composites were lastly synthesized via a simple method at room temperature. The prepared samples are evidently investigated by X-ray powder diffraction, scanning electron microscopy, energy dispersive spectroscopy, ultraviolet-visible diffuse reflectance spectroscopy, photoluminescence spectrum, and X-ray photoelectron spectroscopy, respectively. Using the monochromatic light of ultraviolet, the photocatalytic activity of the TiO_2/CF composites was accurately evaluated with respect to the degradation of an aqueous dye (methylene blue) solution. The relationship between the photocatalytic degradation of methylene blue dye and its ratio, contact time, and the amount of catalyst was studied. The kinetics and mechanisms of degradation were discussed. The results show that TiO_2/CF composites have good photocatalytic activity and stability. The TiO_2/CF2/1 composite was used in effective photocatalytic degradation of methylene blue, the weight ratio of TiO_2 to carbon fiber was 2:1, and the degradation rate was obtaining up to 97.7% of degradation during 120 min of reaction. The photocatalytic stability of TiO_2/CF composites was dependent on the stability of their structure. After 5 repeated uses, the composite TiO_2/CF2/1 still exhibited rather high activity toward the degradation of methylene blue, where the decolorization efficiency of methylene blue achieved 92% and the loss of activity was negligible. Based on radical trapping experiments, the mechanism of TiO_2/CF composites on photocatalytic degradation of methylene blue is proposed, which could explain the enhanced photocatalytic activity of the composites better. Superoxide radicals, photogenerated holes, and photogenerated electrons were the main active substances for methylene blue degradation.

1. Introduction

Water pollution has become a problem of concern in many countries [1–5]. Many dyes in wastewater contain aromatic compounds, which are chemically stable and harmful to human health [6–8]. Due to the adverse effects of these refractory organic compounds on the environment, it is necessary to develop new methods to degrade them. Photocatalysis is a promising technique for the photodegradation of harmful chemicals in wastewater [9–14]. TiO_2 and TiO_2- based nanostructures are being used for photocatalytic degradation of organic pollutants to protect the environment [15–17]. With the advantages of low cost, large specific surface area, high oxidation ability, and good chemical stability, TiO_2 has become one of the most promising candidates for photocatalysis [18]. However, the photocatalytic performance of TiO_2 is severely limited by the large bandgap (3.2 eV) and the high recombination rate of photogenerated electron-hole pairs [19, 20]. On the other hand, the industrial treatment of wastewater containing a variety of organic pollutants using TiO_2-

photocatalysts is not common due to the low photocatalytic activity [21]. In order to solve this problem, several methods have been developed to improve the efficiency of the photocatalytic process of TiO_2, for example, doping, combining with metal oxides, quantum dots, semiconductors, carbon materials, and so on [22–26]. It has been reported that in carbonized PANI/TiO_2 composites, compared with bare anatase TiO_2 nanoparticles, more efficient photo-induced charge separation results in high photogenerated charge carrier mobility and ultimately improves the efficiency of the composite, which can also be explained as the existence of nitrogen in such carbonized nanostructure [27].

During the past twenty years, polyaniline (PANI) has been the most widely studied conductive polymer with good stability, corrosion resistance, nontoxicity, simple and low-cost synthesis method, and high instinctive redox performance, and the research on it eventually won the Nobel Prize Chemistry in 2000 [28]. Particularly, PANI has great potential due to its high absorption coefficients and high mobility of charge carriers. In addition, after the irradiation of light, PANI is not only an electron donor but also an excellent hole acceptor [27]. These special characteristics of PANI make it an ideal material for improving the efficiency of charge separation in the field of photocatalysis. Recently, more and more attention has been focused on the combination of PANI and semiconductor photocatalyst [27, 28]. Zhang et al. and Wang et al. PANI/semiconductor composites were prepared by chemical adsorption and in situ oxidative polymerization, and it was found that the prepared samples had enhanced photocatalytic activity [11, 29].

Composites based on carbonaceous materials and TiO_2 particles usually were synthesized by harsh methods using expensive equipment or at high temperatures [30]. Generally, in these composites, additional interaction of carbonaceous part and TiO_2 nanoparticles was weak, which hinders the effective functionalization of TiO_2 nanoparticles [31]. This article reports for the first time a simple method to synthesize TiO_2/CF composites under room temperature conditions and its photocatalytic performance, to the best of our knowledge. Our method greatly facilitates the synthesis of very effective photocatalytic composites based on TiO_2 nanoparticles and carbon fiber. The structure, morphology, and optical properties of the prepared materials were studied. The photocatalytic activity of TiO_2, CF, and synthetic composites in the degradation of methylene blue dyes was investigated under ultraviolet (UV) light in a comparative study. The relationship between the photocatalytic degradation of methylene blue dye and its ratio, contact time, and the amount of catalyst was studied. In addition, the degradation kinetics and mechanism were also discussed. Also, the stability of the catalyst was studied.

2. Materials and Methods

2.1. Materials. All chemicals applied in this experiment including tetrabutyl titanate (TBT, 99%; Shandong West Asia Chemical Industry Co., Ltd.), acetic acid glacial, polyethylene glycol 400 (PEG 400), and ethanol were purchased and used without any further purification. High-purity deionized water was used throughout all experiments.

2.2. Synthesis of Pure TiO_2 Powder. The pure TiO_2 powder was prepared according to a sol-gel method. In a typical procedure, 10 mL acetic acid glacial, 3.2 mL deionized (DI) water, and 2 mL PEG 400 were firstly dissolved in 20 mL ethanol at room temperature. Then, 20 mL tetrabutyl titanate was secondly dissolved in 40.0 mL ethanol, and it was added dropwise to the above solution under vigorous stirring. Next, the final suspension solution was maintained at 35°C for 2 h under vigorous stirring. The obtained solution was aged at room temperature for 24 h and it was dried at 100°C in an air oven for 10 h. Finally, the obtained sample was ground and calcined at 450°C in an air atmosphere for 2 h with a heating ramp of 10°C/min. The pure TiO_2 powder was obtained.

2.3. Preparation of CF. The polyaniline fiber was calcined at 400°C in a N_2 atmosphere for 2 h with a heating ramp of 5°C/min, and it was ground and stored.

2.4. Synthesis of TiO_2/CF Composites. First, 0.1 g CF was dispersed in a mixture of 20.0 mL ethanol and 5.0 mL DI water. Then, a certain amount of TiO_2 (0.05 g, 0.1 g, 0.2 g, 0.3 g, and 0.4 g) was added and the suspension was left for 2 h under stirring. After that, the suspension was dried for 24 h at 80°C. Hence, the as-prepared composites were named TiO_2/CFx, where x represented the total weight ratio of TiO_2 to CF. Thus, the composites were labeled as follows: TiO_2/CF0.5/1, TiO_2/CF1/1, TiO_2/CF2/1, TiO_2/CF3/1, TiO_2/CF4/1.

2.5. Characterization. The X-ray powder diffraction (XRD) patterns of TiO_2 powder, CF, and the synthetic composites were acquired using a Bruker D8 A25 diffractometer (Cu Kα radiation ($\lambda = 1.5406$ Å), operated at 40 mA and 40 kV) in the 2θ range of 10–90° at a scanning speed of 10°/min. Morphology of TiO_2 powder, CF, and the prepared TiO_2/CF composites were studied using a scanning electron microscope (SEM). Element analysis of the prepared TiO_2/CF composites was studied using an energy dispersive spectroscopy (EDS). The UV-visible diffuse reflectance spectroscopy (UV-vis DRS) and photoluminescence (PL) spectrum of TiO_2 powder, CF, and the synthetic composites were measured by multifunctional optical fiber spectrometer (QE65 Pro, Ocean Optics, USA). The X-ray photoelectron spectroscopy (XPS) of TiO_2 powder, CF, and the synthetic composites were measured by an X-ray photoelectron spectrometer (Thermo escalab 250X).

2.6. Photocatalytic Activity Test. The photocatalytic activity of the photocatalysts was tested by photocatalytic degradation of MB. The photocatalytic tests were carried out under UV-light irradiation at room temperature in an air atmosphere. The TiO_2/CF composites were invited as photocatalysts. The UV light source was generated by a 300 W Mercury lamp. The distance between the photocatalysts and lamp was 10 cm. Before

photocatalytic reaction, 10 mg of prepared photocatalysts was suspended in 50 mL of MB aqueous solution of 5 mg/L. Prior to irradiation, the suspension solutions were stirred magnetically in the dark for 1 h at room temperature in order to reach adsorption-desorption equilibrium between the photocatalysts and MB. After each 20 min irradiation time interval, 4 mL solution of reaction was taken from the suspensions and the photocatalyst was removed by filtered via a 0.45 μm filter membrane (Nylon) for analysis. A UV-vis spectrophotometer at its characteristic wavelength ($\lambda = 664$ nm) was used to measure the absorbance of the residual MB solutions in the solution of reaction. The degradation rate was calculated by C/C_0, where C was the concentration of MB in each time period, and C_0 was the concentration of MB after dark adsorption. In the durability testing, five successive cycles were performed. After each cycle, the photocatalysts were washed with ethanol and DI water carefully and then dried at 60°C for 12 h. Then, the fresh MB dye aqueous solution of 5 mg/L was mixed with the used photocatalysts to carry out the next photocatalytic activity testing.

To identify the generated active species during the reaction process, ammonium oxalate (AO), 1, 4-benzoquinone (BQ), and 2-propanol (IPA) were used as the hole (h^+) scavenger, superoxide radical ($O_2\cdot-$) scavenger, and hydroxyl radical (•OH) scavenger, respectively. The right amount of scavenger was added to the MB dye aqueous solution to probe the active species through variation of degradation rate.

3. Results and Discussion

3.1. Structural Properties. The XRD patterns of TiO_2 powder, CF, and the prepared TiO_2/CF composites are shown in Figure 1. The TiO_2 powder, Figure 1, is composed of anatase as the dominant phase. The main characteristic peaks of TiO_2 anatase at 2theta 25.3°, 37.8°, and 48° are related to (101), (004), and (200) crystal planes, respectively (JCPDS card No. 21–1272) [32]. In addition, other relevant peaks appear at 55° (211) and 62.6° (204) [32]. It is generally known that TiO_2 possesses three types of crystal structure: anatase, brookite, and rutile. Among them, anatase crystals have the highest photocatalytic activity because the oxygen vacancies of anatase crystals are larger than that of brookite crystals and rutile crystals. Furthermore, TiO_2 with anatase crystal form has a low dielectric constant, low mass density, and high electron mobility [33]. For CF, the broad peaks at $2\theta = 17°$ and 43° are designated as characteristic peaks of carbon [27]. For the TiO_2/CF composites, the characteristic peaks of anatase still exist with high intensity, but the characteristic peaks of carbon are not visible in the XRD patterns. This is mainly due to the coverage of anatase crystals on the carbon [28]. In short, a series of composites with anatase crystals were successfully synthesized, indicating that the composites have high photocatalytic activity.

3.2. Morphological Characterization. The surface morphology of TiO_2 powder (a), CF (b), and the prepared TiO_2/CF composites (c) were characterized by SEM images as shown in Figure 2. It could be clearly seen that although some of them

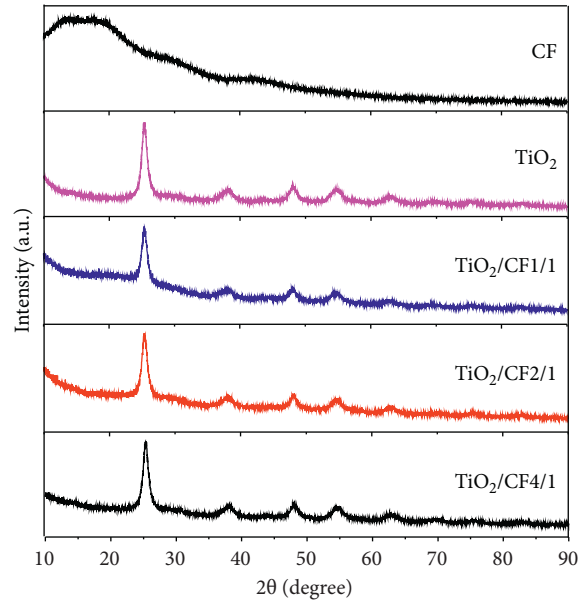

Figure 1: XRD patterns of TiO_2 powder, CF, and the prepared TiO_2/CF composites.

were anatase, the size of the obtained TiO_2 particles was about 100–200 nm. TiO_2 were spherical particles and they were agglomerated. At the same time, it could be seen that TiO_2 was dispersed on CF. The elemental composition of the TiO_2/CF composite was characterized by EDS as shown in Figure 2(d). It could be seen from Figure 2(d) that the prepared TiO_2/CF composite contains Ti, O, and C elements, which were consistent with the results of XPS analysis.

3.3. Optical Properties. The research on the optical properties of TiO_2 powder, CF, and the prepared TiO_2/CF composites is one of the most important parameters affecting the applications of synthetic products. The UV-vis light absorption spectra of TiO_2 powder, CF, and the prepared TiO_2/CF composites are shown in Figure 3. All samples show absorption bands in the visible light region of the spectrum. The composites showed an obvious enhancement of absorption in the visible light band owing to the presence of CF, which helps to enhance the photocatalyst activity [34]. In addition, the absorbance in the visible light band increased as the ratio of CF to TiO_2 increased.

Photoluminescence (PL) spectrum analysis was commonly employed to investigate the separation efficiency of electron-hole pairs. Generally, high photoluminescence intensity corresponds to high electron-hole pairs recombination efficiency, indicating low photocatalytic activity [35]. As shown in Figure 4, when excited with 210 nm UV light, all photocatalysts showed similar emission spectra and had the strongest peak at about 390 nm, which was mainly due to the emission of edgeless excitons [36]. Moreover, it was noted that the intensity of the emission band decreased significantly as the content of TiO_2 increases. According to reports, the decrease of PL intensity was mainly due to three factors [37]: (1) in the presence of TiO_2/CF, photogenerated electrons can be efficiently transferred from TiO_2 to CF, which

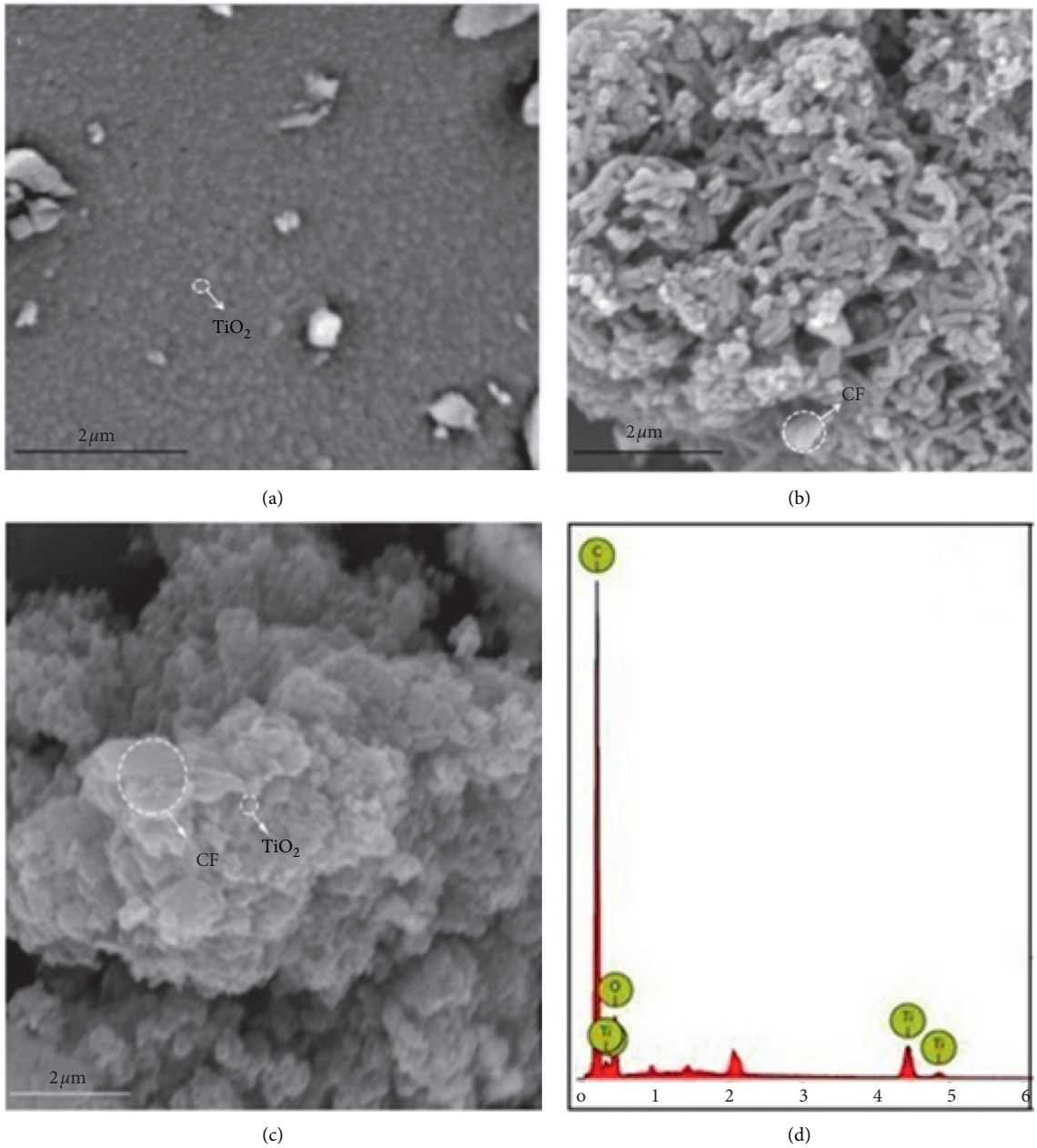

Figure 2: SEM images of (a) TiO_2 powder, (b) CF, and (c) the prepared TiO_2/CF composites, and (d) the EDS of the prepared TiO_2/CF composites.

improves the separation efficiency of electron-hole pairs; (2) the absorbance of photoluminescence caused by CF leads to quenching effect; (3) low-electron light excitation may lead to low-charge recombination. The substantial decrease in the intensity of the PL peak indicates that CF provides the potential to inhibit the recombination of photoelectrons and holes.

3.4. Chemical Compositions. In order to study the chemical composition and interaction between TiO_2 and CF, XPS analysis was used, as shown in Figure 5.

Figure 6 shows the high-resolution XPS spectrum of the C 1s region. The binding energy of 284.8 eV is the typical peak position of the indeterminate carbon pollution absorbed from the surrounding environment and cannot be eliminated [38]. In addition, the deconvolution peaks centered on the binding energies of 286.1 and 288.7 eV were attributed to C-O and C=O oxygen-containing carbon bands, respectively [39]. The C 1s spectrum of TiO_2/CF2/1 is shown in Figure 6(c). The peak intensity at 286.1 eV increases significantly, indicating that C-O bonds were formed in TiO_2/CF2/1. Carbon atoms were bonded to the interstitial positions of the TiO_2 lattice [39].

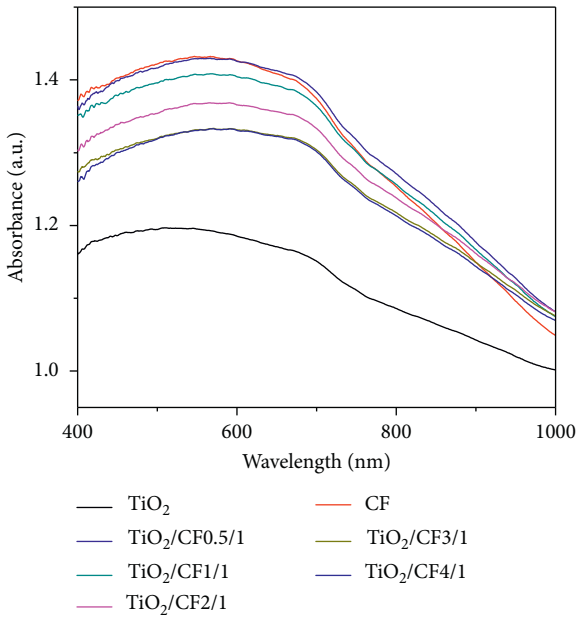

Figure 3: UV-vis absorbance spectra of TiO_2 powder, CF, and the prepared TiO_2/CF composites.

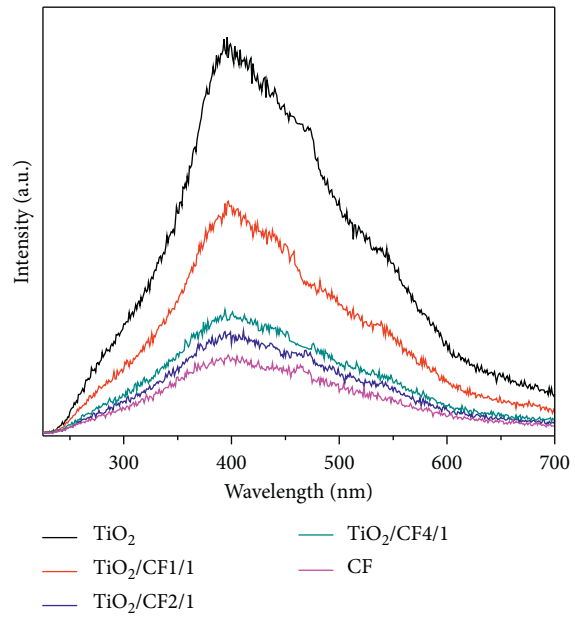

Figure 4: PL spectra of TiO_2 powder, CF, and the prepared TiO_2/CF composites.

Figure 7 shows the high-resolution XPS spectra of the O 1s region of TiO_2 (a) and TiO_2/CF2/1 (b). For pure TiO_2, C-O and O-H bonds centered at 532.8 eV and 531.2 eV were found, respectively [40]. The O 1s spectrum of TiO_2/CF2/1 was shown in Figure 7(b). The peak intensities at 532.8 eV and 531.2 eV increase significantly, indicating that C-O and O-H bonds were formed in TiO_2/CF2/1; that is, oxygen atoms were incorporated into the TiO_2 crystal lattice the gap position [40].

Figure 8 shows the high-resolution XPS spectra of the N 1s region of CF (a) and TiO_2/CF2/1 (b). For the CF in

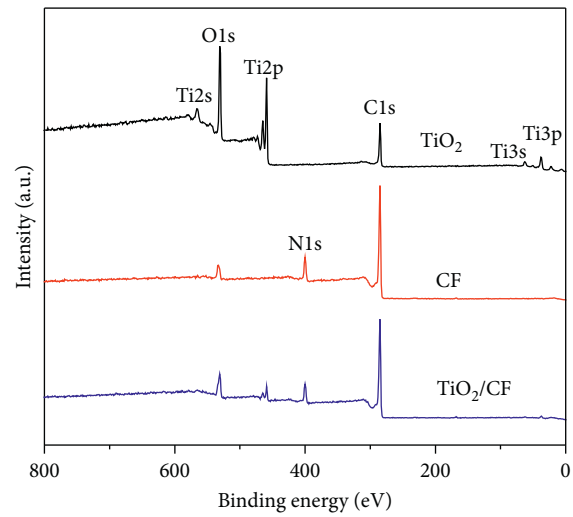

Figure 5: XPS spectra: survey spectrum.

Figure 8(a), there were three corresponding characteristic peaks. The peak at 398.5 eV was attributed to the C=N-C group, while the other peaks at 399.6 eV and 400.9 eV could be attributed to N-$(C)_3$ and the N-H group [41]. Therefore, it shows that the double bond of N=C had been broken, and both the nitrogen atom and the carbon atom were bonded to the titanium atom, resulting in the formation of the N-Ti-C group. In comparison with CF, there were only three peaks attributed to CF in TiO_2/CF2/1 as shown in Figure 8(b).

As shown in Figure 9, the formation of C-Ti bonds and N-Ti bonds in TiO_2/CF2/1 also could be further checked and confirmed by analyzing the Ti 2p core level of XPS. For pure TiO_2, Ti $2p_{3/2}$ and Ti $2p_{1/2}$ with 458.8 eV and 464.5 eV as the centers were found, which were assigned to the Ti-O bond [42]. In Figure 9(b), in addition to the two characteristic peaks of TiO_2, which were 458.8 (Ti $2p_{3/2}$) and 464.5 eV (Ti $2p_{1/2}$), two other peaks could be found, located at 462.1 eV and 456.9 eV, respectively and were determined to be caused by the N-Ti bond, and the remaining peak at 460.8 eV was attributed to the C-Ti bond [43]. This indicates that there were N-Ti bonds and C-Ti bonds in TiO_2/CF2/1.

Combined with the above analysis, two additional bonds (N-Ti bond and C-Ti bond) were formed in TiO_2/CF2/1, which indicates that TiO_2 nanoparticles were chemically bonded to CF in TiO_2/CF2/1.

3.5. Photocatalytic Activity. Figure 10(a) shows the photocatalytic performance of TiO_2 powder, CF, and the prepared TiO_2/CF composites based on MB degradation under UV light irradiation. The results show that pure TiO_2 has photocatalytic activity under UV light irradiation. Moreover, all TiO_2/CF composites exhibit excellent photocatalytic activity, and their activity was higher than that of a single component. When the mass ratio of TiO_2/CF was 2 : 1 (TiO_2/CF2/1), the photocatalytic activity was the best, and the MB removal rate reaches 97.7% after 2 hours of reaction.

Photocatalytic degradation follows first-order kinetics. Kinetics can be expressed as follows:$-\ln(C/C_0) = k_{app}\, t$.

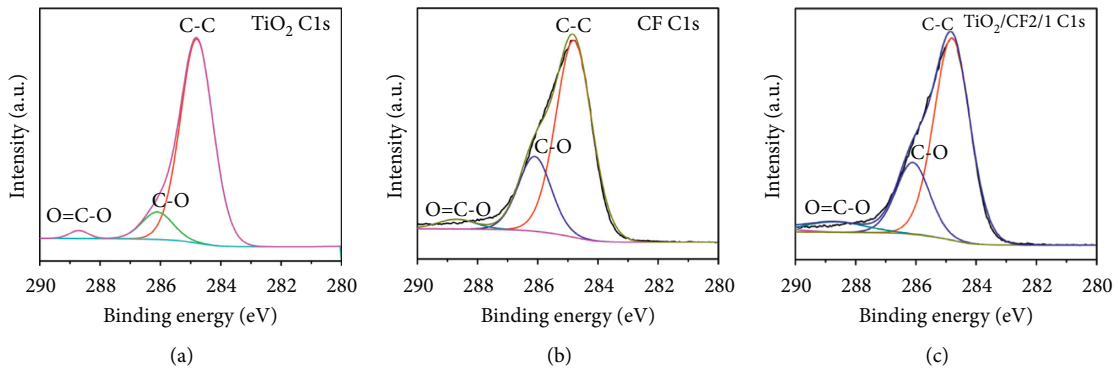

Figure 6: C 1s XPS spectra of (a) TiO_2, (b) CF, and (c) TiO_2/CF2/1.

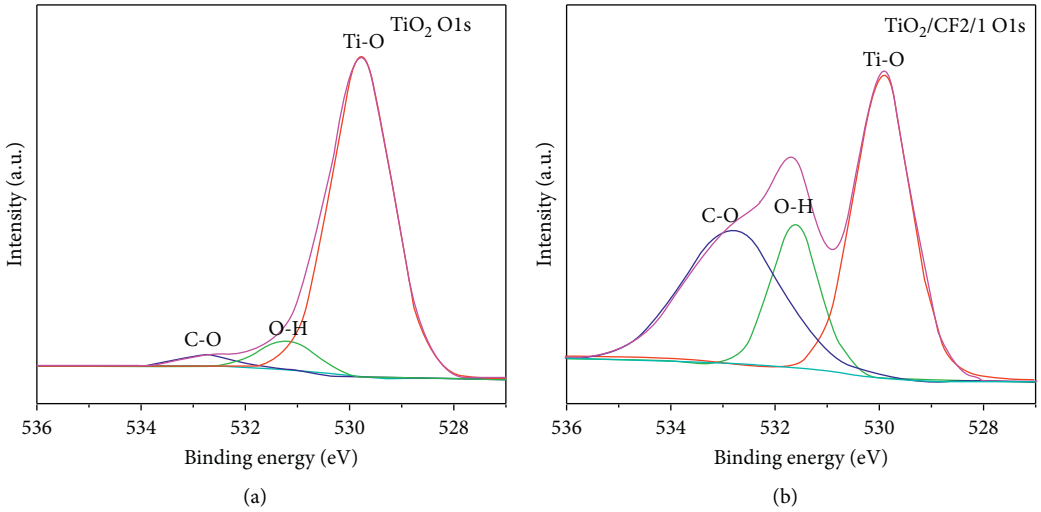

Figure 7: O 1s XPS spectra of (a) TiO_2 and (b) TiO_2/CF2/1.

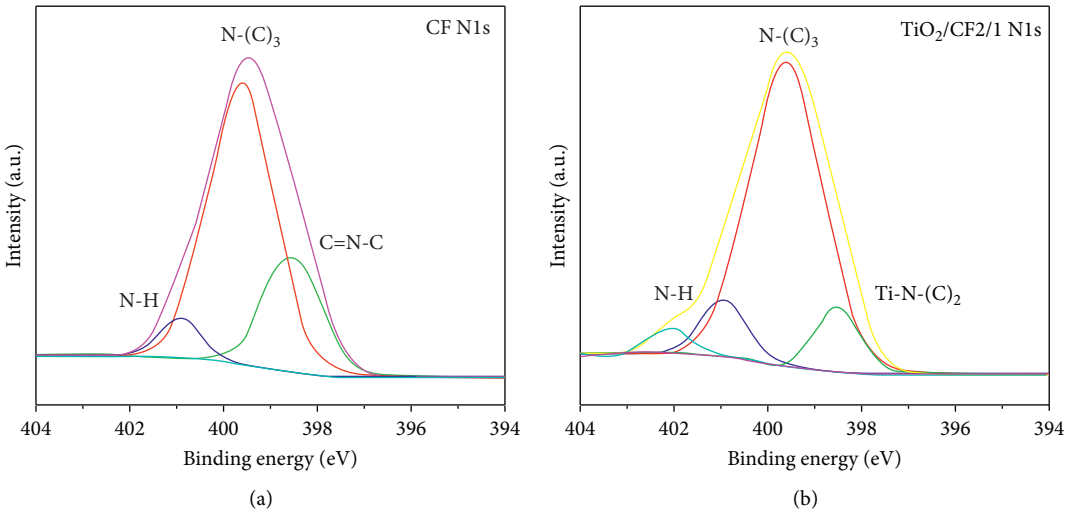

Figure 8: N 1s high-resolution XPS spectra of (a) CF and (b) TiO_2/CF2/1.

Figure 10(b) shows the linear relationship between ln (C/C_0) and time, where C/C_0 was normalized to the MB concentration, t was the reaction time, and k was the reaction rate constant (10^{-3} min^{-1}). Figure 10(c) shows the reaction rate constants for TiO_2 powder, CF, and the prepared TiO_2/CF composites. The rate constant of TiO_2/CF2/1 was calculated

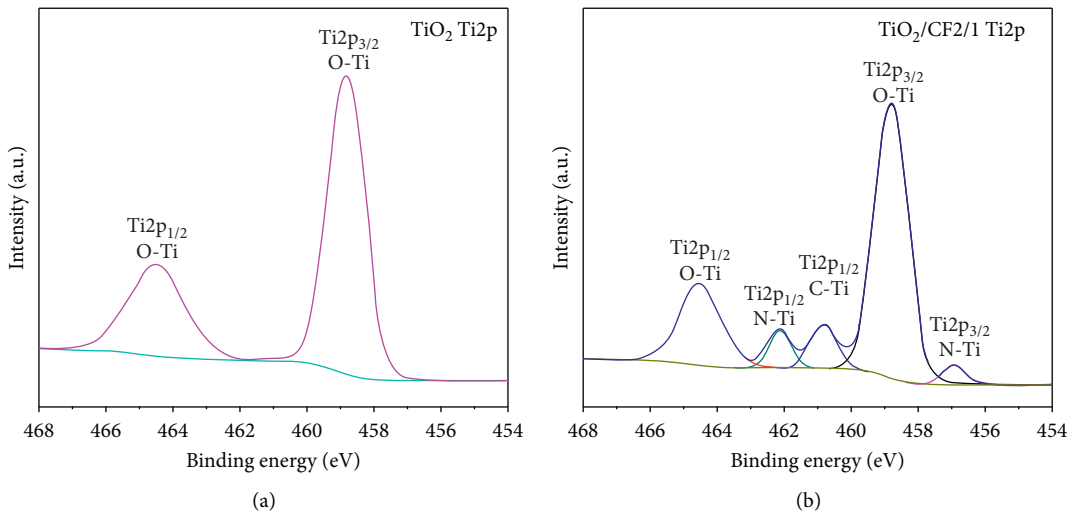

Figure 9: Ti 2p high-resolution XPS spectra of (a) TiO_2 and (b) TiO_2/CF2/1.

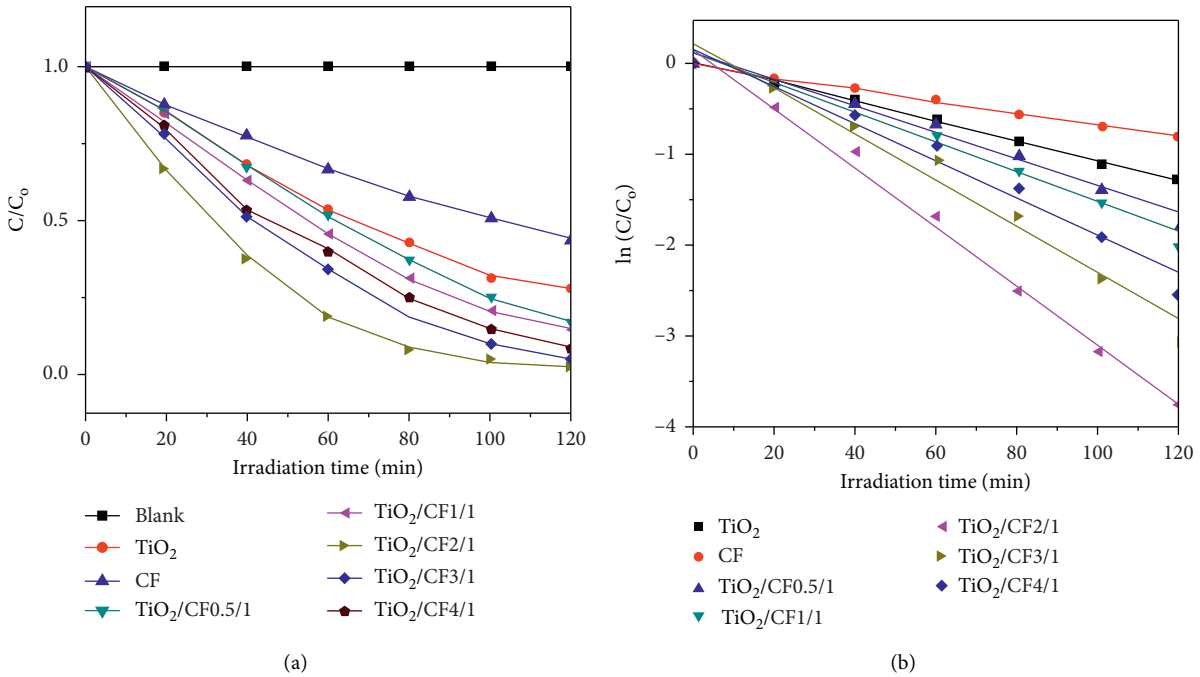

Figure 10: Continued.

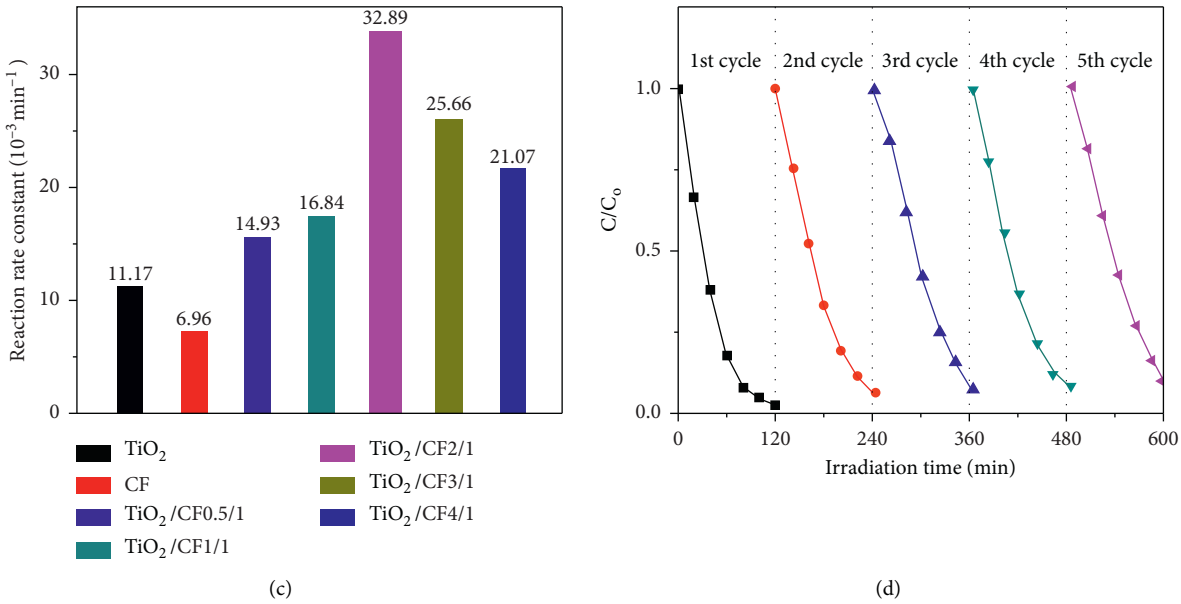

Figure 10: (a) The photocatalytic degradation rate of MB when TiO_2 powder, CF, and the prepared TiO_2/CF composites were irradiated under UV light for 2 h; (b) kinetic curves of photocatalytic degradation of TiO_2 powder, CF, and the prepared TiO_2/CF composites; (c) reaction rate constants of TiO_2 powder, CF and the prepared TiO_2/CF composites; (d) study on the stability of TiO_2/CF2/1 photocatalytic degradation MB.

to be 0.03289 min^{-1}, which was 2.9 times and 4.7 times higher than that of TiO_2 and CF, respectively. Therefore, it was believed that effectively separating electron-hole pairs through chemical bond connection can greatly improve the photocatalytic activity of UV light photocatalyst.

For the practical application of the photocatalyst, the stability of the photocatalyst was one of the key issues. The by-products were always adsorbed on the surface active sites of the photocatalyst. The photocatalytic activity will drop sharply after a short period of exposure time. In order to evaluate the stability of the prepared TiO_2/CF2/1, a cycle experiment was carried out under the same conditions. According to the results shown in Figure 10(d), TiO_2/CF2/1 still showed exhibits excellent photocatalytic performance in the fifth cycle.

In this study, the effect of the dosage on the MB removal efficiency of the TiO_2/CF composites was studied at the same MB concentration by varying its doses from 5 to 20 mg or 0.15 to 0.25 g/L. Figure 11 shows that using an appropriate amount of photocatalyst can increase the removal rate of MB and then reach equilibrium. The degradation efficiency of MB increased significantly to 97.7% as the dose increased from 5 to 20 mg or 0.15 to 0.25 g/L after 2 hours of reaction. This indicates other active sites of the photocatalyst for MB adsorption. Using CF to functionalizing TiO_2 into composites will increase the adsorption capacity of TiO_2 because of its extra surface area.

Although the physical and chemical interaction between MB and TiO_2/CF2/1 may increase its surface coverage, after reaching the optimal dose, its particles will gather in TiO_2/CF2/1 clusters, shielding UV light from interacting with the active surface of the photocatalyst. Therefore, this situation reduces the generation of ·OH. Other studies had also reported that a dose of 10 mg or 0.20 g/L was optimum for MB degradation [44, 45].

In order to further explore the role of photo-active species in the reaction process, the relevant scavengers were added to the MB solution by comparing the changes in the degradation rate. As shown in Figure 12, it clearly shows that the degradation rate was significantly reduced after adding AO, BQ, and IPA. And the degradation rate follows the following order: no scavenger > AO > IPA > BQ. Therefore, it can be known that h^+, O2·− and •OH, which were active substances, were generated in the photocatalytic reaction, and O2·− plays a very important role.

3.6. Mechanism Discussion. Based on the above analysis and discussion, it could be concluded that the improvement of light collection between TiO_2 and CF was the main factor for improving the photocatalytic activity. As shown in Scheme 1, when the TiO_2/CF composites were irradiated with UV light, electrons were excited from the VB to the CB of TiO_2 and CF, leaving holes in the VB. Since the CB of CF was much higher than that of TiO_2, and the VB of CF was located at a higher position than that of TiO_2, the excited electrons were transferred from the CB of CF to the CB of TiO_2, and the holes migrate in the opposite direction. Moreover, CF loading with TiO_2 could facilitate charge transport, hinder the recombination of electron-hole pairs, and further increase the number of charge carriers in the reaction [28]. Therefore, the TiO_2/CF composites exhibit better photocatalytic activity.

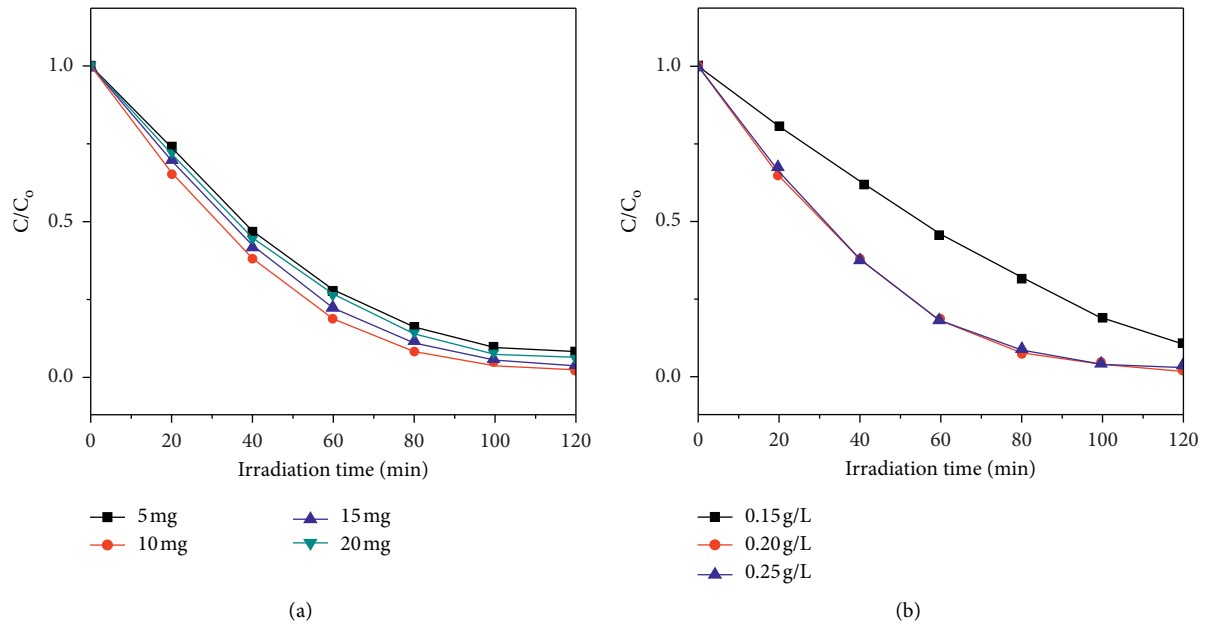

Figure 11: The effect of photocatalyst dosage (a) and concentration (b) on MB removal under UV light irradiation.

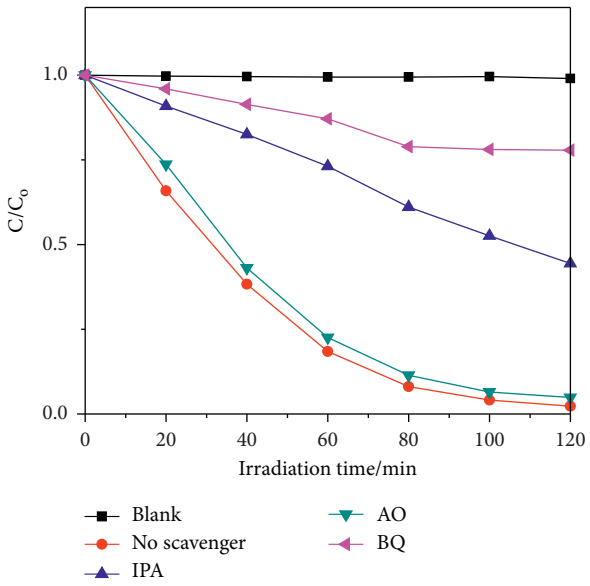

Figure 12: Photodegradation rate of MB after different scavengers were added.

Based on the scavenger experiment, combined with the above-mentioned mechanism analysis, O2·− was the main role in the photocatalytic reaction produced by the reduction of O_2 in CB of TiO_2. And •OH was formed by the further reaction of O2·−, e^-, and $2H^+$. The photocatalytic process could be represented by the following process:

$$TiO_2/CF \text{ composites} + UV \longrightarrow CF\ (h^+) + TiO_2\ (e^-)$$

$$O_2 + e^- \longrightarrow O2\cdot-$$

$$O2\cdot- + e^- + 2H^+ \longrightarrow H_2O_2;$$

$$H_2O_2 + e^- \longrightarrow \bullet OH + OH^- + O_2$$

$$O2\cdot-/\bullet OH/h^+ + MB \longrightarrow CO_2 + H_2O/\text{degraded products}$$

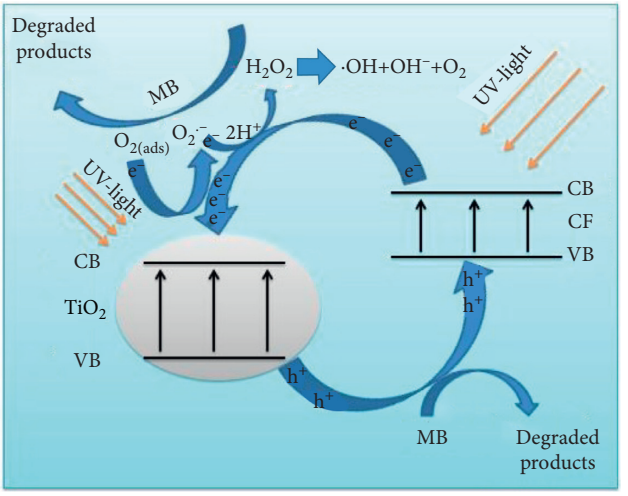

Scheme 1: Mechanism diagram of photocatalytic reaction of MB under UV-light.

4. Conclusions

In summary, the TiO_2/CF composites with high photocatalytic activity were successfully synthesized by a simple method at room temperature. The MB photodegradation performance of TiO_2/CF composites was better than that of TiO_2 or CF under the same conditions in the photocatalytic system under UV light irradiation. And the optimum mass ratio of TiO_2 to CF was 2 : 1. The stability test of the photocatalyst shows that TiO_2/CF2/1 had high stability and the photodegradation efficiency after the fifth cycle was 92%. SEM showed that TiO_2 particles grew well on the surface of CF. XPS shows that TiO_2 particles were chemically bonded to CF, which was confirmed by the formation of C-Ti bonds and N-Ti bonds. This chemical bonding structure was conducive to the formation of an effective heterojunction,

which might lead to the synergistic combination of TiO_2 and CF, thereby significantly reducing the recombination of electron-hole pairs and enhancing the separation of photogenerated carriers. It was also proved by the PL spectrum. Since O2·− and ·OH free radicals were generated in the TiO_2/CF/UV system, it could degrade up to 97.70% of MB. In addition, scavenger experiments show that O2·− was the main role participating in photocatalytic activity. The existence of these free radicals was confirmed by free radical suppression tests using different scavengers for different free radicals. This study shows that simple TiO_2/CF composites were efficient and promising photocatalysts for dye degradation in water.

Data Availability

All data used to support this study are included within the paper.

Conflicts of Interest

The authors declare no conflicts of interest.

Authors' Contributions

Hao Cheng and Wenkang Zhang authors contributed equally to this work.

Acknowledgments

This work was supported by the National Natural Science Foundation of China (no. 21968005), the Opening Project of Guangxi Key Laboratory of Clean Pulp and Papermaking and Pollution Control (KF201812-4), and the High Levels of Innovation Team and Excellence Scholars Program in Colleges of Guangxi.

References

[1] M. Shaban, A. M. Ashraf, and M. R. Abukhadra, "TiO_2 Nanoribbons/carbon nanotubes composite with enhanced photocatalytic activity; fabrication, characterization, and application," *Scientific Reports*, vol. 8, p. 781, 2018.

[2] M. R. A. Kumar, B. Abebe, H. P. Nagaswarupa et al., "Enhanced photocatalytic and electrochemical performance of TiO_2-Fe_2O_3 nanocomposite: its applications in dye decolorization and as supercapacitors," *Scientific Reports*, vol. 10, p. 1249, 2020.

[3] F. Ouyang, H. Li, and B. Bharti, "Photocatalytic degradation of industrial acrylonitrile wastewater by F-S-Bi-TiO_2 catalyst of ultrafine nanoparticles dispersed with SiO_2 under natural sunlight," *Scientific Reports*, vol. 10, Article ID 12379, 2020.

[4] Z. Feng, L. Zeng, Q. L. Zhang et al., "In situ preparation of g-C_3N_4/$Bi_4O_5I_2$ complex and its elevated photoactivity in Methyl orange degradation under visible light," *Journal of Environmental Sciences*, vol. 87, pp. 149–162, 2020.

[5] X. M. Liu, Y. Liu, W. K. Zhang, Q. Y. Zhong, and X. Y. Ma, "In situ self-assembly of 3D hierarchical 2D/2D CdS/g-C_3N_4 hereojunction with excellent photocatalytic performance," *Materials Science in Semiconductor Processing*, vol. 105, Article ID 104734, 2020.

[6] L. Gao, W. Gan, Z. Qiu et al., "Preparation of heterostructured WO_3/TiO_2 catalysts from wood fibers and its versatile photodegradation abilities," *Scientific Reports*, vol. 7, no. 1102, 2017.

[7] X. Gao, X. Liu, Z. Zhu et al., "Enhanced visible light photocatalytic performance of CdS sensitized TiO_2 nanorod arrays decorated with Au nanoparticles as electron sinks," *Scientific Reports*, vol. 7, p. 973, 2017.

[8] W. K. Zhang, Q. Y. Zhong, X. M. Liu, and Q. Lu, "Inorganic functionalization of $CdSe_xS_{1-x}$/ZnS core-shell quantum dots and their photoelectric properties," *Physica Status Solidi (A) Applications and Materials Science*, vol. 217, Article ID 2000010, 2020.

[9] A. Makhatova, G. Ulykbanova, S. Sadyk et al., "Degradation and mineralization of 4-tert-butylphenol in water using Fe-doped TiO_2 catalysts," *Scientific Reports*, vol. 9, Article ID 19284, 2019.

[10] X. Guo, J. Dai, K. Zhang, X. Wang, Z. Cui, and J. Xiang, "Fabrication of N-doped TiO_2/activated carbon fiber composites with enhanced photocatalytic activity," *Textile Research Journal*, vol. 84, no. 17, pp. 1891–1900, 2014.

[11] D. Zhang, T. Cong, L. Xia, and L. Pan, "Growth of black TiO_2 nanowire/carbon fiber composites with dendritic structure for efficient visible-light-driven photocatalytic degradation of methylene blue," *Journal of Materials Science*, vol. 54, no. 10, pp. 7576–7588, 2019.

[12] L. Chen, W. Q. Zhang, J. F. Wang et al., "High piezo/photocatalytic efficiency of Ag/Bi_5O_7I nanocomposite using mechanical and solar energy for N_2 fixation and methyl orange degradation," *Green Energy & Environment*, vol. 4, no. 9, 2021.

[13] S. D. Perera, R. G. Mariano, K. Vu et al., "Hydrothermal synthesis of graphene-TiO_2 nanotube composites with enhanced photocatalytic activity," *Acs Catalysis*, vol. 2, no. 6, pp. 949–956, 2012.

[14] W. Q. Zhang, P. X. Xing, J. Y. Zhang et al., "Facile preparation of novel nickel sulfide modified $KNbO_3$ heterojunction composite and its enhanced performance in photocatalytic nitrogen fixation," *Journal of Colloid and Interface Science*, vol. 590, pp. 548–560, 2021.

[15] X. M. Liu, F. I. Chowdhury, L. J. Meng et al., "Luminescent films employing quantum dot-cellulose nanocrystal hybrid nanomaterials," *Materials Letters*, vol. 294, Article ID 129737, 2021.

[16] Y. Q. Cao, T. Q. Zi, X. R. Zhao et al., "Enhanced visible light photocatalytic activity of Fe_2O_3 modified TiO_2 prepared by atomic layer deposition," *Scientific Reports*, vol. 10, Article ID 13437, 2020.

[17] P. F. Chen, L. Chen, S. F. Ge et al., "Microwave heating preparation of phosphorus doped g-C_3N_4 and its enhanced performance for photocatalytic H_2 evolution in the help of Ag_3PO_4 nanoparticles," *International Journal of Hydrogen Energy*, vol. 45, no. 28, pp. 14354–14367, 2020.

[18] Y. Wen, H. Ding, and Y. Shan, "Preparation and visible light photocatalytic activity of Ag/TiO_2/graphene nanocomposite," *Nanoscale*, vol. 3, no. 10, pp. 4411–4417, 2011.

[19] W. Yao, B. Zhang, C. Huang, C. Ma, X. Song, and Q. Xu, "Synthesis and characterization of high efficiency and stable Ag_3PO_4/TiO_2 visible light photocatalyst for the degradation of methylene blue and rhodamine B solutions," *Journal of Materials Chemistry*, vol. 22, no. 9, pp. 4050–4055, 2012.

[20] R. Leary and A. Westwood, "Carbonaceous nanomaterials for the enhancement of TiO_2 photocatalysis," *Carbon*, vol. 49, no. 3, pp. 741–772, 2011.

[21] B. Chen, Y. Meng, J. Sha, C Zhong, W Hu, and N Zhao, "Preparation of MoS_2/TiO_2 based nanocomposites for photocatalysis and rechargeable batteries: progress, challenges, and perspective," *Nanoscale*, vol. 10, no. 1, pp. 34–68, 2017.

[22] X. D. Zhu, Y. J. Wang, R. J. Sun, and D. M. Zhou, "Photocatalytic degradation of tetracycline in aqueous solution by nanosized TiO_2," *Chemosphere*, vol. 92, no. 8, pp. 925–932, 2013.

[23] S. Fu, G. W. Wang, M. Wang, Y. Wang, C. H. Xia, and H. G. Zhang, "Design of TiO_2 nanocrystals with enhanced sunlight photocatalytic activity by exploring calcining conditions," *Ceramics International*, vol. 46, no. 13, pp. 21268–21274, 2020.

[24] C. Chen, W. Cai, M. Long et al., "Synthesis of visible-light responsive graphene oxide/TiO_2 composites with p/n heterojunction," *ACS Nano*, vol. 4, no. 11, pp. 6425–6432, 2010.

[25] A. Ajmal, I. Majeed, R. N. Malik et al., "Principles and mechanisms of photocatalytic dye degradation on TiO_2 based photocatalysts: a comparative overview," *Cheminform*, vol. 45, pp. 37003–37026, 2015.

[26] W. Li, D. Li, Y. Lin et al., "Evidence for the active species involved in the photodegradation process of methyl orange on TiO_2," *The Journal of Physical Chemistry C*, vol. 116, no. 5, pp. 3552–3560, 2012.

[27] K. R. Reddy, V. G. Gomes, and M. Hassan, "Carbon functionalized TiO_2 nanofibers for high efficiency photocatalysis," *Materials Research Express*, vol. 1, Article ID 15012, 2014.

[28] Y. M. Lin, D. Z. Li, J. H. Hu et al., "Highly efficient photocatalytic degradation of organic pollutants by PANI-modified TiO_2 composite," *The Journal of Physical Chemistry C*, vol. 116, no. 9, pp. 5764–5772, 2012.

[29] R. Marija, M. Gordana, S. Vuk et al., "Superior photocatalytic properties of carbonized PANI/TiO_2 nanocomposites," *Applied Catalysis B: Environmental*.vol. 213, pp. 155–166, 2017.

[30] D. H. Wang, L. Jia, X. L. Wu, L. Q. Lu, and A. W. Xu, "One-step hydrothermal synthesis of N-doped TiO_2/C nanocomposites with high visible light photocatalytic activity," *Nanoscale*, vol. 4, no. 2, pp. 576–584, 2012.

[31] R. Daghrir, P. Drogui, and D. Robert, "Modified TiO_2 for environmental photocatalytic applications: a review," *Industrial & Engineering Chemistry Research*, vol. 52, pp. 3581–3599, 2013.

[32] A. Fujishima, X. Zhang, and D. A. Tryk, "TiO_2 photocatalysis and related surface phenomena," *Surface Science Reports*, vol. 63, pp. 515–582, 2008.

[33] C. Dette, M. A. Perez-Osorio, C. S. Kley et al., "TiO_2 anatase with a bandgap in the visible region," *Nano Letters*, vol. 14, pp. 6533–6538, 2014.

[34] W. Zhou, H. Liu, J. Wang et al., "Ag_2O/TiO_2 nanobelts heterostructure with enhanced ultraviolet and visible photocatalytic activity," *Acs Applied Materials & Interfaces*, vol. 2, pp. 2385–2392, 2010.

[35] S. Bai, L. Wang, X. Chen et al., "Chemically exfoliated metallic MoS_2 nanosheets: a promising supporting co-catalyst for enhancing the photocatalytic performance of TiO_2 nanocrystals," *Nano Research*, vol. 8, pp. 175–183, 2015.

[36] B. Cheng, Y. Le, and J. Yu, "Preparation and enhanced photocatalytic activity of Ag@TiO_2 core-shell nanocomposite nanowires," *Journal of Hazardous Materials*, vol. 177, pp. 971–977, 2010.

[37] Y. Liang, H. Wang, H. S. Casalongue et al., "TiO_2 nanocrystals grown on graphene as advanced photocatalytic hybrid materials," *Nano Research*, vol. 3, pp. 701–705, 2010.

[38] K. Nakata and A. Fujishima, "TiO_2 photocatalysis: design and applications," *Journal of Photochemistry and Photobiology C: Photochemistry Reviews*.vol. 13, pp. 169–189, 2012.

[39] M. Ge, C. Cao, J. Huang et al., "A review of one-dimensional TiO_2 nanostructured materials for environmental and energy applications," *Journal of Materials Chemistry A*, vol. 4, pp. 6772–6801, 2016.

[40] M. A. Henderson, "A surface science perspective on TiO_2 photocatalysis," *Surface Science Reports*, vol. 66, pp. 185–297, 2011.

[41] S. Y. Lee and S. J. Park, "TiO_2 photocatalyst for water treatment applications," *Journal of Industrial and Engineering Chemistry*, vol. 19, pp. 1761–1769, 2013.

[42] D. P. Macwan, P. N. Dave, and S. Chaturvedi, "A review on nano-TiO_2 sol-gel type syntheses and its applications," *Journal of Materials Science*, vol. 46, pp. 3669–3686, 2011.

[43] G. Liu, L. C. Yin, J. Wang et al., "A red anatase TiO_2 photocatalyst for solar energy conversion," *Energy & Environmental Science*.vol. 5, pp. 9603–9610, 2012.

[44] T. Ochiai and A. Fujishima, "Photoelectrochemical properties of TiO_2 photocatalyst and its applications for environmental purification," *Journal of Photochemistry and Photobiology C: Photochemistry Reviews*, vol. 13, pp. 247–262, 2012.

[45] Y. C. Pu, G. Wang, K. D. Chang et al., "Au nanostructure-decorated TiO_2 nanowires exhibiting photoactivity across entire UV-visible region for photoelectrochemical water splitting," *Nano Letters*, vol. 13, p. 3817, 2013.